Paediatric and adult soft tissue sarcomas with NTRK1 gene fusions: a subset of spindle cell sarcomas unified by a prominent myopericytic/haemangiopericytic pattern

Florian Haller, Jasmin Knopf, Anne Ackermann, Matthias Bieg, Kortine Kleinheinz, Matthias Schlesner, Evgeny A Moskalev, Rainer Will, Ali Abdel Satir, Ibtihalat E Abdelmagid, Johannes Giedl, Roman Carbon, Oliver Rompel, Arndt Hartmann, Stefan Wiemann, Markus Metzler, Abbas Agaimy

Angaben zur Veröffentlichung / Publication details:

Haller, Florian, Jasmin Knopf, Anne Ackermann, Matthias Bieg, Kortine Kleinheinz, Matthias Schlesner, Evgeny A Moskalev, et al. 2016. "Paediatric and adult soft tissue sarcomas with NTRK1 gene fusions: a subset of spindle cell sarcomas unified by a prominent myopericytic/haemangiopericytic pattern." *The Journal of Pathology* 238 (5): 700–710. https://doi.org/10.1002/path.4701.

Paediatric and adult soft tissue sarcomas with *NTRK1* gene fusions: a subset of spindle cell sarcomas unified by a prominent myopericytic/haemangiopericytic pattern

Florian Haller,[1]* Jasmin Knopf,[1] Anne Ackermann,[1] Matthias Bieg,[2] Kortine Kleinheinz,[2] Matthias Schlesner,[2] Evgeny A Moskalev,[1] Rainer Will,[3] Ali Abdel Satir,[4] Ibtihalat E Abdelmagid,[5] Johannes Giedl,[1] Roman Carbon,[6] Oliver Rompel,[7] Arndt Hartmann,[1] Stefan Wiemann,[3,8] Markus Metzler[9] and Abbas Agaimy[1]

[1] *Institute of Pathology, University Hospital, Friedrich-Alexander University Erlangen-Nuremberg, Erlangen, Germany*
[2] *Division of Theoretical Bioinformatics (B080), German Cancer Research Centre (DKFZ), Heidelberg, Germany*
[3] *Genomics and Proteomics Core Facility, German Cancer Research Centre (DKFZ), Heidelberg, Germany*
[4] *HistoCentre, Khartoum, Sudan*
[5] *National Public Health Laboratory, Khartoum, Sudan*
[6] *Department of Paediatric Surgery, University Hospital, Friedrich-Alexander University Erlangen-Nuremberg, Erlangen, Germany*
[7] *Department of Radiology, University Hospital, Friedrich-Alexander University Erlangen-Nuremberg, Erlangen, Germany*
[8] *Division Molecular Genome Analysis, German Cancer Research Centre (DKFZ), Heidelberg,*
[9] *Department of Paediatrics, University Hospital, Friedrich-Alexander University Erlangen-Nuremberg, Erlangen, Germany*

**Correspondence to: F Haller or A Agaimy, Institute of Pathology, University Hospital, Friedrich-Alexander University Erlangen-Nuremberg, Erlangen, Germany. E-mail: florian.haller@uk-erlangen.de; abbas.agaimy@uk-erlangen.de*

Abstract

Neoplasms with a myopericytomatous pattern represent a morphological spectrum of lesions encompassing myopericytoma of the skin and soft tissue, angioleiomyoma, myofibromatosis/infantile haemangiopericytoma and putative neoplasms reported as malignant myopericytoma. Lack of reproducible phenotypic and genetic features of malignant myopericytic neoplasms have prevented the establishment of myopericytic sarcoma as an acceptable diagnostic category. Following detection of a *LMNA–NTRK1* gene fusion in an index case of paediatric haemangiopericytoma-like sarcoma by combined whole-genome and RNA sequencing, we identified three additional sarcomas harbouring *NTRK1* gene fusions, termed 'spindle cell sarcoma, NOS with myo/haemangiopericytic growth pattern'. The patients were two children aged 11 months and 2 years and two adults aged 51 and 80 years. While the tumours of the adults were strikingly myopericytoma-like, but with clear-cut atypical features, the paediatric cases were more akin to infantile myofibromatosis/haemangiopericytoma. All cases contained numerous thick-walled dysplastic-like vessels with segmental or diffuse nodular myxohyaline myo-intimal proliferations of smooth muscle actin-positive cells, occasionally associated with thrombosis. Immunohistochemistry showed variable expression of smooth muscle actin and CD34, but other mesenchymal markers, including STAT6, were negative. This study showed a novel variant of myo/haemangiopericytic sarcoma with recurrent *NTRK1* gene fusions. Given the recent introduction of a novel therapeutic approach targeting *NTRK* fusion-positive neoplasms, recognition of this rare but likely under-reported sarcoma variant is strongly encouraged.

Keywords: NTRK1; sarcoma; myopericytic sarcoma; haemangiopericytoma; infantile fibrosarcoma

Introduction

Historically, the term 'haemangiopericytoma' (HPC) has been applied non-specifically to a variety of benign low- and high-grade neoplasms with a prominent pericytic growth pattern. Through the years, however, the rubric of HPCs underwent continuous critical reappraisal in which, as a first step, specific types of sarcoma (eg synovial sarcoma and osteosarcoma) with the presence of a HPC-like pattern have been eliminated [1]. This was followed by the merging of HPC and solitary fibrous tumour (SFT) into a single unified entity, which has been confirmed recently by the universal presence of *NAB2–STAT6* gene fusions in these tumours [2,3]. Nonetheless, in a previous study we reported on specific histomorphological and clinical features of classical fibrous and cellular variants of tumours within the family of SFT/HPC that were characterized by distinct variants of the *NAB2–STAT6* fusion gene [4]. Moreover, we observed that sinonasal HPC (glomangiopericytoma) lacks the *NAB2–STAT6* gene fusion [5] and instead harbours activating

mutations of β-*catenin* [6]. However, there has still been a group of intermediate or high-grade neoplasms characterized by prominent HPC- or myopericytoma-like features but lacking other characteristic phenotypic or genetic markers. Some examples of the latter have been reported as malignant myopericytoma [7].

In the current study, we employed combined whole-genome and RNA sequencing to decipher the molecular genetic background of an unclassified huge deep-seated paediatric infantile HPC-like neoplasm that we diagnosed hypothetically as the malignant counterpart of infantile myofibromatosis (haemangiopericytic or myopericytic sarcoma). This tumour was negative for the *ETV6–NTRK3* gene fusion defining congenital/infantile fibrosarcoma [8]. Of note, we observed a gene fusion involving the genes encoding Lamin A/C (*LMNA*) and neurotrophic tyrosine kinase receptor, type 1 (*NTRK1*). Subsequently, we identified three additional histologically malignant tumours within our archival and consultation files with overlapping features of HPC/myopericytoma comprising paediatric and adult patients. Two cases harboured *TPM3–NTRK1* fusions, with the fourth case showing a combined *NTRK1* fusion event with amplification. Based on our pilot study, we propose that *NTRK1* gene fusions may be a recurrent event among tumours presenting with features of myo/haemangiopericytic sarcoma. In the context of recently introduced specific therapeutic approaches addressing tumours with *NTRK1* gene fusions [9,10], our observation represents a first clue to which sarcomas would need to be tested to achieve a reasonable frequency of positive cases in clinical routine diagnostic setting.

Materials and methods

Patients and tumour samples

This study was approved by the local ethics committee of the University Hospital Erlangen, Germany (No. 217_12 B, 19.09.2012). Signed informed consent was obtained from all participating patients (or their parents in the two paediatric cases) in this study. The index case (Case 1) was treated surgically at our institution. Fresh-frozen tumour tissue was obtained from the resection specimen and a peripheral blood sample from the patient as well. A second paediatric case was retrieved by searching for *ETV6–NTRK3* gene fusion-negative paediatric sarcomas that were initially thought to represent congenital/infantile fibrosarcoma (the only such case in our archives). Two adult cases with a hypothetical diagnosis of 'spindle cell sarcoma, NOS with prominent myopericytic pattern' were identified from the consultation files of one of the authors (AA).

Immunohistochemistry

All tumour specimens had been fixed in buffered formalin overnight and processed routinely for histological assessment. Immunohistochemistry, on 3 µm sections cut from paraffin blocks, was performed using a fully automated Benchmark XT System (Ventana Medical Systems, Tucson, AR, USA) and the following antibodies: pan-cytokeratin (clone AE1/AE3, 1:40, Zytomed); CK7 (OV-TL, 1:1000, Biogenex); vimentin (V9, 1:100, Dako); desmin (clone D33, 1:250, Dako); α-smooth muscle actin (clone 1A4, 1:200, Dako); h-caldesmon (clone h-CD, 1:100, Dako); protein S-100 (polyclonal, 1:2500, Dako); CD34 (clone BI-3C5, 1:200, Zytomed); ERG (EPR3864, prediluted, Ventana); myogenin (clone F5D, 1:50, Dako); and STAT6 (clone sc-621, 1:1000, Santa Cruz Biotechnology, Santa Cruz, CA, USA).

Whole-genome sequencing of the index case

Tumour DNA and normal DNA as a control were isolated from fresh-frozen tumour tissue and blood using the DNeasy Blood and Tissue Kit (Qiagen, Hilden, Germany), respectively, and the quality of the DNA was analysed using a 2200 TapeStation (Agilent, Waldbronn, Germany). A total load of 1 µg DNA was fragmented (E220; Covaris, Woburn, MA, USA) and size selected to 300 base pairs (bp), using an E-Gel system (Life Technologies, Darmstadt, Germany) for library preparation, employing the TruSeq Nano DNA Library Prep Kit (Illumina, San Diego, CA, USA) according to the manufacturer's instructions. Paired-end sequencing (2 × 150 bp) was performed using one lane of a HiSeqX (Illumina) for every sample, and a total of 947 486 689 and 883 744 130 non-duplicate reads were mapped for tumour DNA and normal DNA, respectively, to obtain a mean coverage of > 30×. Alignment of whole-genome sequencing reads, SNV calling and identification of translocations were performed as described in detail previously [6]. Additionally, absolute copy numbers for genomic segments were estimated using the allele-specific copy number estimation using next generation sequencing (ACEseq) pipeline (Kortine Kleinheinz; presented as a talk at the Cancer Genomics EMBL Conference, EMBL Heidelberg, Germany, 4 November 2015). The estimation is based on the coverage ratio of tumour and control and on the B-allele frequency (BAF) of SNP positions.

RNA-seq of the index case

RNA was isolated of fresh-frozen tumour tissue using the RNeasy Plus Mini Kit (Qiagen), and quality of RNA was assessed with an Agilent Bioanalyser 2100 (Agilent). Library preparation for RNA-seq was performed using the Illumina TruSeq RNA Sample Preparation Kit v. 2 (Illumina), according to the manufacturer's instructions. A total amount of 1 µg total RNA was fragmented to a median length of 150 bp (Covaris), and 154 935 526 non-duplicate reads were mapped after paired-end sequencing (2 × 100 bp), employing a HiSeq2000 (Illumina). Alignment of RNA-sequencing reads, detection of gene fusions and determination of RPKM values (reads/kb transcript/million mapped reads) were performed as described in detail recently [6].

NTRK1 and *CDKN2A* fluorescence *in situ* hybridization (FISH)

To detect alterations of the *NTRK1* gene locus, FISH was performed on freshly cut sections from formalin-fixed, paraffin-embedded (FFPE) tissue blocks, using the ZytoLight SPEC NTRK1 Dual Color Break Apart Probe (ZytoVision GmbH, Bremerhaven, Germany) with standard protocols according to the manufacturer's instructions; 50 tumour cells were visually inspected using a fluorescence microscope. A cut-off of > 20% tumour cells with aberrant signals was used to classify samples as *NTRK1*-rearranged. Additionally, the Urovysion bladder cancer kit (Abott Laboratories, Des Plaines, IL, USA) was used to analyse the *CDKN2A* gene locus at 9p21.3. All cases were independently scored by two pathologists (FH and JG) and revealed concordant results.

RT–PCR for detection of *LMNA–NTRK1* and *TPM3–NTRK1* gene fusions

RNA was isolated from freshly cut sections of FFPE tissue blocks using an RNeasy FFPE kit and deparaffinization solution (Qiagen). Approximately 700 ng total RNA was used for cDNA synthesis (Quantitect reverse transcription kit, Qiagen). Forward primers located in *LMNA* exon 3 and *TPM3* exons 6–8 were combined with reverse primers in *NTRK1* exons 8–11 to amplify specific PCR products only when the compatible gene fusion was present (see supplementary material, Tables S1, S2). PCR products were visualized on a 2.5% agarose gel stained with ethidium bromide.

LMNA–NTRK1 expression constructs and drug treatment

The open reading frame of the *LMNA–NTRK1* fusion was synthesized and cloned into pUC57–KAN plasmid at Genewiz (South Plainfield, USA). The fusion consisted of *LMNA* exons 1–3 at the 5′ end, followed by *NTRK1* exons 10–16 at the 3′ end. The fusion was shuttled from the pUC57–KAN plasmid into a modified lentiviral expression vector pCDH under the control of a constitutive EF1 promoter (System Biosciences, Mountain View, USA), using Gateway technology (ThermoFisher, Braunschweig, Germany). After propagation, the endotoxin-free construct (EndoFree Plasmid Maxi Kit, Qiagen) was employed for the generation of pseudoviral particles in HEK293T cells (Dulbecco's modified Eagle's medium supplemented with 10% fetal bovine serum and 5% sodium pyruvate) according to the manufacturer's protocol (System Biosciences); 200 µl of crude viral supernatant supplemented with 5 µg/ml polybrene was added to 2×10^5 CCD-33Lu or CCD-1137Sk cells. Cell viability was assessed using the resazurin assay (Sigma-Aldrich, St. Louis, MO, USA). For drug treatment, 1500 cells/well were seeded in 96-well plates 24 h prior to treatment with AZ-23 (AxonMedchem, Groningen, The Netherlands) and CEP-701 (Sigma-Aldrich) at concentrations of 1, 10, 100 and 1000 nM. Resazurin was added 72 h after drug treatment, as described before. The lentiviral expression vector pLenti X2 Hygro/shp16 (w192-1) was a gift from Eric Campeau (Addgene plasmid no. 22264). The endotoxin-free plasmid was used to generate pseudoviral particles in HEK293T cells, as described above. Viral supernatant (400 µl) supplemented with 5 µg/ml Polybrene were added to 2×10^5 CCD-33Lu or CCD-1137Sk cells in six-well plates. The multiplicity of infection (MOI) was quantified using the hygromycin B (Sigma-Aldrich) resistance in the plasmid; 400 µl viral supernatant was the concentration at which > 50% of the seeded cells died and the remaining cells after 7 days of hygromycin B selection were further propagated. Efficiency of $p16^{INK4A}$ knockdown was assessed using qRT–PCR with gene-specific primers, and revealed > 100-fold reduction in $p16^{INK4A}$ mRNA expression (data not shown; primers and protocol are available on request).

Protein isolation and western blotting

Protein lysates were isolated from snap-frozen tumour samples and cell pellets. A total of 15 µg/sample was separated by electrophoresis in 7.5% polyacrylamide gel electrophoresis (PAGE), followed by transfer onto a nitrocellulose membrane. For detection, anti-TrkA antibody (ab76291, 1:1000 dilution; Abcam, Cambridge, UK), anti-PLCγ1 antibody (no. 2822, 1:1000 dilution, Cell Signaling Technology, Danvers, USA), anti-phospho-PLCγ1 (Tyr783) antibody (no. 2821, 1:1000 dilution, Cell Signaling Technology) and anti-rabbit antibody (111-036-045, 1:5000 dilution; Jackson ImmunoResearch Laboratories, West Grove, USA) were used in combination with anti-ACTB (1:5000 dilution, Sigma-Aldrich; anti-mouse antibody, 1:5000 dilution, 115-036-062, Jackson ImmunoResearch Laboratories) serving as loading control. SuperSignal West Femto Maximum Sensitivity Substrate and Pierce ECL Western Blotting Substrate (ThermoFisher Scientific, Waltham, USA) were respectively used for the detection of the target proteins and ACTB.

Results

Detection and functional characterization of the *LMNA–NTRK1* gene fusion in an unclassified huge deep-seated paediatric infantile HPC-like neoplasm (haemangiopericytic/myopericytic sarcoma)

Whole-genome sequencing of the index case revealed a deletion of 739 842 bp at chromosomal region 1q22-23.1 (hg 19, chr1: 156 104 511–156 844 352), with breakpoint mapping within intron 3 of *LMNA* and intron 9 of *NTRK1*. Correspondingly, RNA-seq confirmed an in-frame fusion transcript of 5′ exons 1–3 of LMNA fused to 3′ exons 10–16 of *NTRK1*. The predicted chimeric fusion protein consisted of a

N-terminal part with two coiled-coil domains of LMNA, and a C-terminal part with a transmembrane domain and the complete kinase domain of NTRK1 (Figure 1A). Both genomic breakpoint and the presence of an in-frame fusion transcript were validated by Sanger sequencing, using genomic DNA and RNA/cDNA, respectively, from the patient's tumour sample as template (Figure 1B, C). Separate plotting of the RNA-seq RPKM values of each *NTRK1* exon displayed an ~100-fold increase in RPKM values for exons 10–16, characteristic of a 3′ fusion gene (Figure 1D). Western blot analysis using a monoclonal antibody directed against the C-terminal region of NTRK1/TrkA identified a band in the patient's tumour sample corresponding to the predicted size of 66 kDa of the LMNA–NTRK1 fusion protein that was not present in a case of infantile myofibromatosis (MF) or two SFTs serving as negative controls (Figure 1E). Copy number variation analysis according to the whole-genome sequencing data revealed gains of whole chromosomes 8, 11, 12 and 20, as well as deletions at chromosomal regions 4p15.2–4p15.1 and 9p (see supplementary material, Figure S1). Notably, detailed analysis of the deletion at 9p showed a heterozygous loss of chromosomal region chr9:15 086 470–33 645 001 with additional loss of chromosomal region chr9:19 608 955–22 995 483, resulting in complete homozygous loss of the gene locus *CDKN2A* at 9p21.3 encoding for the cell cycle inhibitors $p16^{INK4A}$ and $p14^{ARF}$. Western blot analysis of lung and skin fibroblasts ectopically expressing the LMNA–NTRK1 fusion construct revealed a strong expression of the LMNA–NTRK1 fusion protein in the skin fibroblasts, resulting in an activation of phospholipase Cγ1 (PLCG1) (Figure 2A). The activation of PLCG1 is consistent with a previously reported model of a LMNA–NTRK1 gene fusion construct ectopically expressed in melan-a cells [11]. Treatment of skin fibroblasts ectopically expressing the LMNA–NTRK1 fusion construct with two TrkA inhibitors demonstrated a reasonable activity of CEP-701 at the range of 10–100 nM, whereas AZ-23 showed no significant activity (Figure 2B).

Detection of *NTRK1* gene fusions in three additional soft tissue sarcomas with pericytic growth pattern

We employed a *NTRK1* break-apart probe for FISH analysis of the *NTRK1* gene locus in the index case and three additional soft tissue sarcomas with pericytic growth pattern (Table 1). The index case harbouring the *LMNA–NTRK1* gene fusion, and in accordance with the chromosomal deletion at 1q22-23.1, displayed one single red signal mapping to the 3′ part of *NTRK1* combined with a loss of the green signal mapping to the 5′ region of *NTRK1* (Figure 3A). Two cases displayed a break-apart signal with close proximity of the red and green probes (Figure 3B, D), consistent with *TPM3–NTRK1* gene fusions, according to an inversion within the long arm of chromosome 1 previously reported in papillary thyroid cancer [12], KM12 cells [13] and soft tissue sarcoma [9]. RT–PCR confirmed *TPM3–NTRK1* gene fusions in both cases (see supplementary material, Figure S2). The fourth case showed ~10 red signals with loss of the green signals, corresponding to a *NTRK1* gene fusion with additional amplification of the fusion gene locus (Figure 3C). RT–PCR to identify the 5′ fusion partner gene was not feasible, owing to insufficient RNA quality in this consultation case referred from a peripheral hospital. Five cases of sporadic infantile myofibromatosis were additionally tested by FISH, and none of these cases harboured a *NTRK1* rearrangement. Furthermore, FISH analysis employing the Urovysion bladder cancer probe set revealed loss of the *CDKN2A* gene locus located at chromosomal region 9p21.3 in the three cases with simple *NTRK1* gene fusions, whereas the case with amplification of the *NTRK1* fusion gene displayed two intact copies of the *CDKN2A* gene locus (Table 1). Lung fibroblasts transduced with the *LMNA–NTRK1* fusion construct at one copy/cell displayed no difference in cell viability compared to the vector control, whereas the same cells with additional transient p16 knock-out showed ~two-fold increased viability comparable to lung fibroblasts transduced with the *LMNA–NTRK1* fusion construct at ~15 copies/cell (Figure 3E).

Pathological features of *NTRK1* fusion-positive soft tissue sarcomas

The main clinicopathological features of the four cases are summarized in Table 1. Representative images illustrating radiological and gross features of the index case (Case 1) are shown in Figure S3 (see supplementary material). Tumour sizes were in the range 3–14 cm, with all but one tumour measuring ≥ 6 cm in maximum diameter. Histological examination after extensive sampling of larger tumours and whole embedding of smaller ones showed two distinctive patterns that were correlated with paediatric and adult tumours, respectively. Among the two paediatric cases, one (the index case) showed areas closely mimicking cellular areas of infantile myofibromatosis but merging with highly cellular fascicles of spindle cells with clear-cut atypical features, infiltrative growth and high mitotic activity of 12/10 high-power fields (HPFs) (Figure 4). A prominent haemangiopericytomatous communicating vasculature lacking any recognizable vascular wall was seen throughout the tumour (Figure 4A, B). A remarkable feature of this case was the frequent occurrence of nodular myo-intimal proliferations of smooth muscle actin-positive cells originating from the vessel wall (Figure 4C) that were occasionally bordered by osteoclastic giant cells (Figure 4D). These nodules, however, never showed coalescence or formed dense aggregates as seen in typical myofibromatosis. The second paediatric case was a nondescript spindle cell neoplasm that closely resembled low-grade myofibroblastic sarcoma (Figure 4E) but with a variable myofibromatosis-like vasculature in the periphery. Again, scattered osteoclastic-like giant cells were seen, as in the index case (Figure 4F). Mitotic activity was high, with 17/10 HPFs. In close relation but also

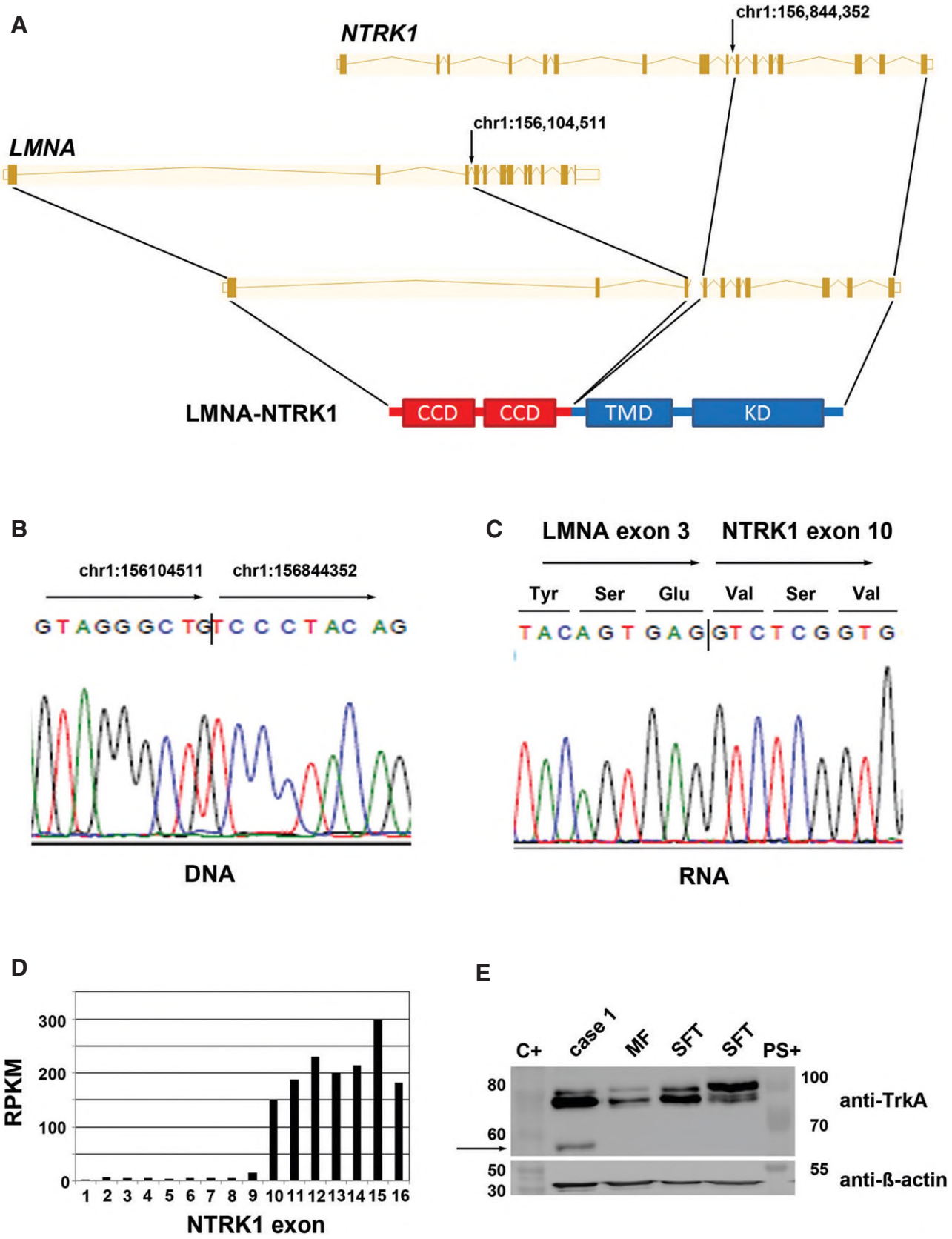

Figure 1. Combined whole-genome and RNA sequencing identifies a *LMNA–NTRK1* gene fusion in a paediatric infantile HPC-like neoplasm. (A) Schematic presentation of the *LMNA–NTRK1* gene fusion with breakpoints in intron 3 of *LMNA* and intron 9 of *NTRK1*. (B) Confirmation of the genomic breakpoint by Sanger sequencing. (C) Confirmation of the corresponding in-frame fusion transcript at the RNA/cDNA level. (D) Note the ~100-fold increase of RPKM values for NTRK1 exons 10–16 after the breakpoint. (E) Western blot displays the aberrant fusion protein in the index patient sample (Case 1) at the predicted size of +66 kDa (arrow), whereas three control samples (MF, infantile myofibromatosis; SFT, solitary fibrous tumour) display only the wild-type NTRK1/TrkA protein at ~87 kDa

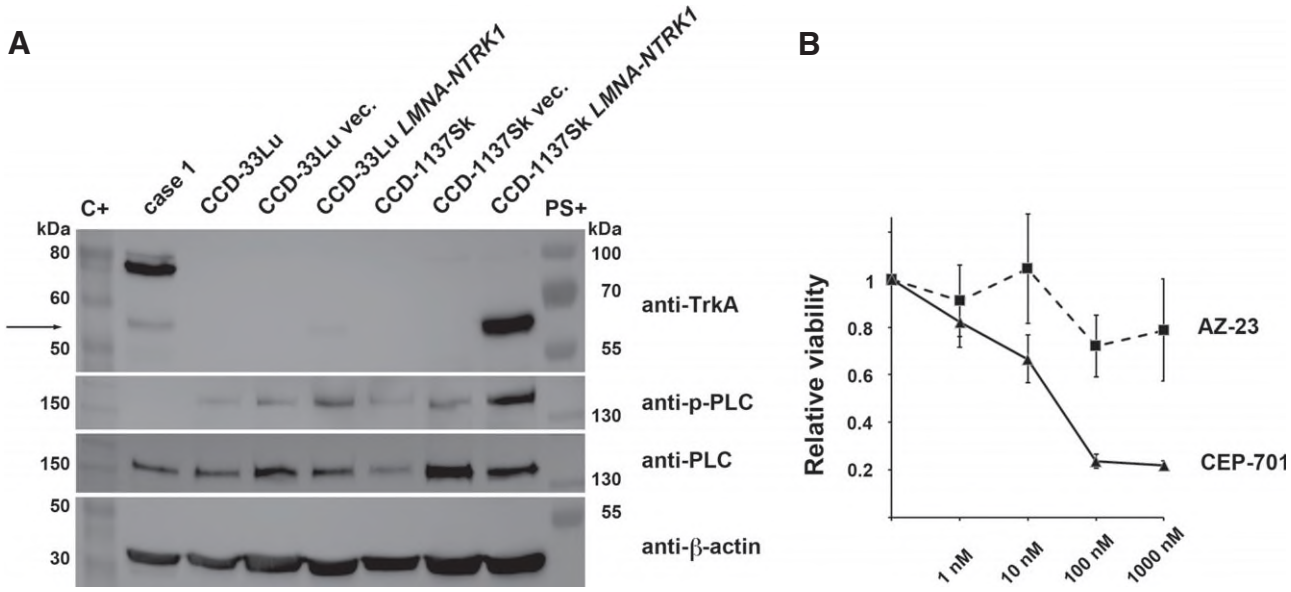

Figure 2. LMNA–NTRK1 fusion activates phospholipase Cγ1 (PLCG1) *in vitro* and can be targeted with the TrkA inhibitor CEP-701. (A) The LMNA–NTRK1 fusion construct was ectopically expressed in lung and skin fibroblasts: skin fibroblasts expressing the LMNA–NTRK1 fusion (arrow) show increased activation of PLCG1 compared to empty vector or lung fibroblasts without demonstrable LMNA–NTRK1 fusion expression. (B) Relative viability (vertical axis) is plotted for *LMNA–NTRK1*-transduced skin fibroblasts that are treated with increasing concentrations of the TrkA inhibitors AZ-23 and CEP-701 (horizontal axis): cell viability was estimated by the resazurin assay; the viability of the vehicle-treated cells was set to 1; error bars indicate SD. Note a significant reduction of cell viability at concentrations of 10–100 nM CEP-701

distinct from these features observed in the paediatric tumours were the adult cases (Case 3, Figure 5A–D; Case 4, Figure 5E–F). Both adult cases showed highly cellular areas composed of fibroblast-like nondescript spindle cells with tapering nuclei, indistinctive nucleoli and pale eosinophilic cytoplasm set within a variably fibrous to myxoid-oedematous stroma. A prominent myopericytic pattern was seen that ranged from small rounded vascular spaces surrounded by onion skin-like arrangements of tumour cells, reminiscent of myopericytoma, to perivascular tumour cell condensation superficially mimicking the pattern seen in some malignant peripheral nerve sheath tumours. A common feature seen in both cases was the presence of plump epithelioid-looking tumour cells with eosinophilic cytoplasm and peripherally located, occasionally bilobed, nuclei with a plasmacytoid cell appearance, usually closely associated with the vascular walls or in perithelial location (Figure 5C, D). These cells occasionally showed mitotic figures. Communicating sinusoidal-like vascular gaps, as seen in haemangiopericytoma-like neoplasms, were seen in both cases and were very prominent in one case. Mitotic activity was 14 and 16 mitotic figures/10 HPFs in the two cases. Atypical mitoses were seen in one case (Case 3). Some tumour vessels had segmental or diffuse wall thickening, with atypical tumour cells seen throughout the vascular wall. These vessels frequently showed variable degrees of thrombotic occlusions of the vascular lumens. Immunohistochemistry showed highly variable and mainly focal reactivity for CD34 in one adult case (Table 1). One paediatric case showed diffuse cytoplasmic expression of ASMA, while the other cases were negative except for the myo-intimal nodular proliferations. Notably, none of the four cases showed residual foci of typical infantile-type myofibroma or contained residual benign myopericytoma as a possible precursor lesion.

Discussion

Based on histomorphological, immunohistochemical and clinical features, the majority of spindle cell neoplasms in childhood represent tumours in the spectrum of infantile myofibromatosis/infantile HPC and congenital/infantile fibrosarcoma [14,15]. Activating germline mutations in the genes *PDGFRB* and *NOTCH3* were reported in familial myofibromatoses [16,17] and somatic gain-of-function mutations of *BRAF* were recently observed in myopericytomas [18]. On the other hand, infantile fibrosarcoma is defined genetically by recurring *ETV6–NTRK3* gene fusions [8]. However, a group of paediatric spindle cell tumours with haemangio/myopericytic features, but lacking the above genetic alterations, are occasionally encountered. In the current study, we report on gene fusions of *NTRK1* in four tumours demonstrating morphological features of infantile HPC and myopericytic sarcoma in two children and two adults, respectively.

Regarding our paediatric cases, it could be argued that these are not really sarcomas, as none has metastasized to date. Of note, a recent study by Linos *et al* [19] described atypical features in 24/226 infantile myofibromas that were reported as sarcomas by most of the submitting pathologists. Their cases carried superficial

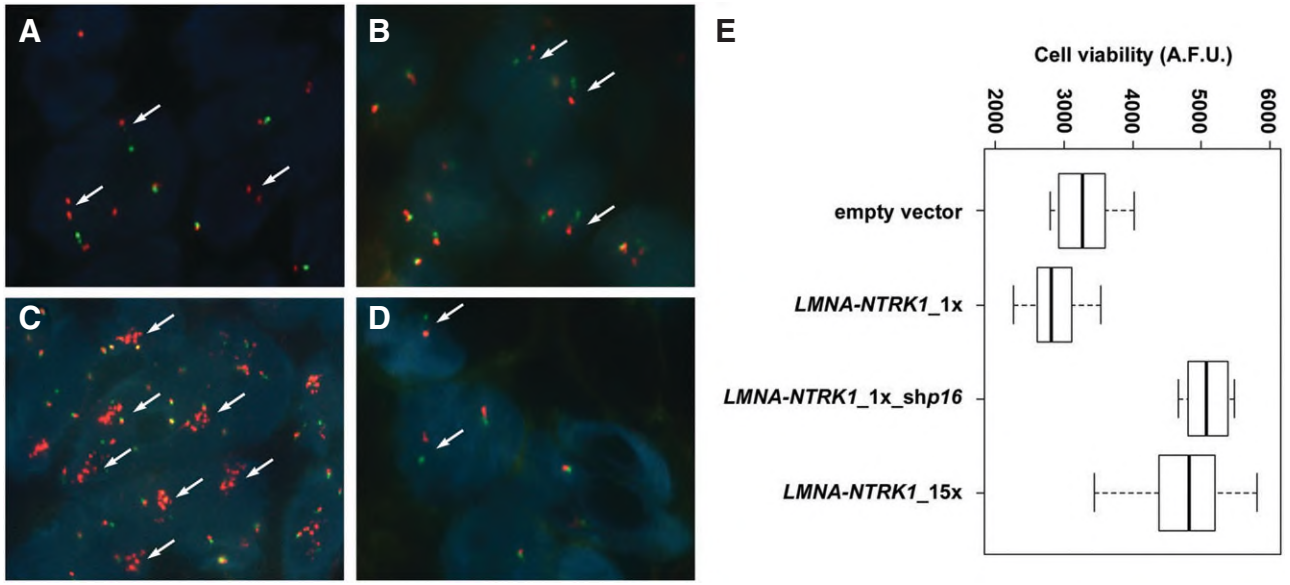

Figure 3. Fluorescence *in situ* hybridization using a *NTRK1* break-apart probe confirms *NTRK1* gene fusions in the index case and identifies three additional cases. (A) Index case (Case 1) with *LMNA–NTRK1* gene fusion according to 740 kb deletion at chromosome 1q, showing a single red signal corresponding to the 3′-region of *NTRK1* gene locus. (B) Case 2 with split signals of the 5′- (green) and 3′- (red) regions of the *NTRK1* gene locus in close proximity, corresponding to an intrachromosomal inversion. RT–PCR confirmed a *TPM3–NTRK1* fusion in this case. (C) This tumour (Case 3) showed >10 *NTRK1* 3′-region split signals (red), indicating a combined genetic aberration with amplification of a translocated *NTRK1* fusion gene involving the NTRK1 kinase domain. (D) Case 4 with split signals and a pattern similar to case 2. This case also harboured a *TPM3–NTRK1* fusion confirmed by RT–PCR. (E) Cell viability evaluated by resazurin assay (A.F.U., arbitrary fluorescence units) is shown for lung fibroblasts. Note essentially no difference in viability between the cells transduced with *LMNA–NTRK1* fusion constructs at ~ one copy/cell and the vector control, but substantial increase of viability upon additional knock-down of p16 or transduction at ~15 copies/cell

similarity to our paediatric cases, suggesting that our two paediatric cases might represent myofibromatoses with atypical features. However, several differences existed between their and our cases, including deep location, absence of prominent or confluent myoid nodules or areas of typical myofibroma, lack of actin expression in one tumour, significantly larger tumour size and a higher mitotic activity (14 and 17 versus 5/10 HPFs) in our cases. Most importantly, both our cases lacked *PDGFRB* mutations (data not shown). Unfortunately, the *PDGFRB* status was not reported in the series of Linos *et al* [19]. Based on these differences, we argue that our cases do not represent atypical myofibromatoses but should rather be considered as low-grade sarcomas. Nevertheless, their definitive biology remains to be assessed as more genetically similar cases are reported in the future. It should be pointed out, however, that rare myofibromatosis-like paediatric lesions have been reported that metastasized > 10 years later as myosarcomas [20]. Thus, we cannot judge from the available follow-up the definitive malignant potential of such rare neoplasms.

Regarding our adult cases, both showed histological features of tumours reported previously as malignant myopericytoma, and this was essentially the putative original diagnosis in both cases. However, reported malignant myopericytoma seems to follow an aggressive course, with metastases occurring in four of five patients, of which three patients died within 1 year [7]. The unremarkable course of one of our cases (no metastases at 29 months) indicates a less aggressive neoplasm. Furthermore, both our cases lacked any actin immunoreactivity, in contrast to the previous series on malignant myopericytoma. This difference in tumour course might be related to the presence of several adverse features in the series of McMenamin and Fletcher [7], where their tumours had a median mitotic rate of 27/10 HPFs, showed frequent foci of necrosis and contained atypical mitoses. However, despite the high degree of histomorphological architectural and cellular homology between their and our two adult tumours, one cannot ascertain from histology alone whether their cases belong to the same genetic entity as ours.

The family of tropomyosin-receptor kinases (Trk) comprises three paralogous members, TrkA, TrkB and TrkC, encoded by the gene loci *NTRK1*, *NTRK2* and *NTRK3*, respectively. Physiologically, the Trk kinase family members play important roles in the development of the central and peripheral nervous system, and are involved in the regulation of cell proliferation, differentiation, apoptosis and survival of neurons [21]. Originally observed in a case of colorectal cancer [22], gene fusions involving the 3′ region of *NTRK1* are frequently present in a subset of papillary thyroid carcinomas [12]. Recently, next-generation sequencing studies reported on rare cases with *NTRK1* gene fusions in non-small cell lung cancers [13], glioblastomas [23], paediatric gliomas [24], spitzoid naevi/melanomas [11] and soft tissue sarcomas [9,25]. Recurrent 5′ partner

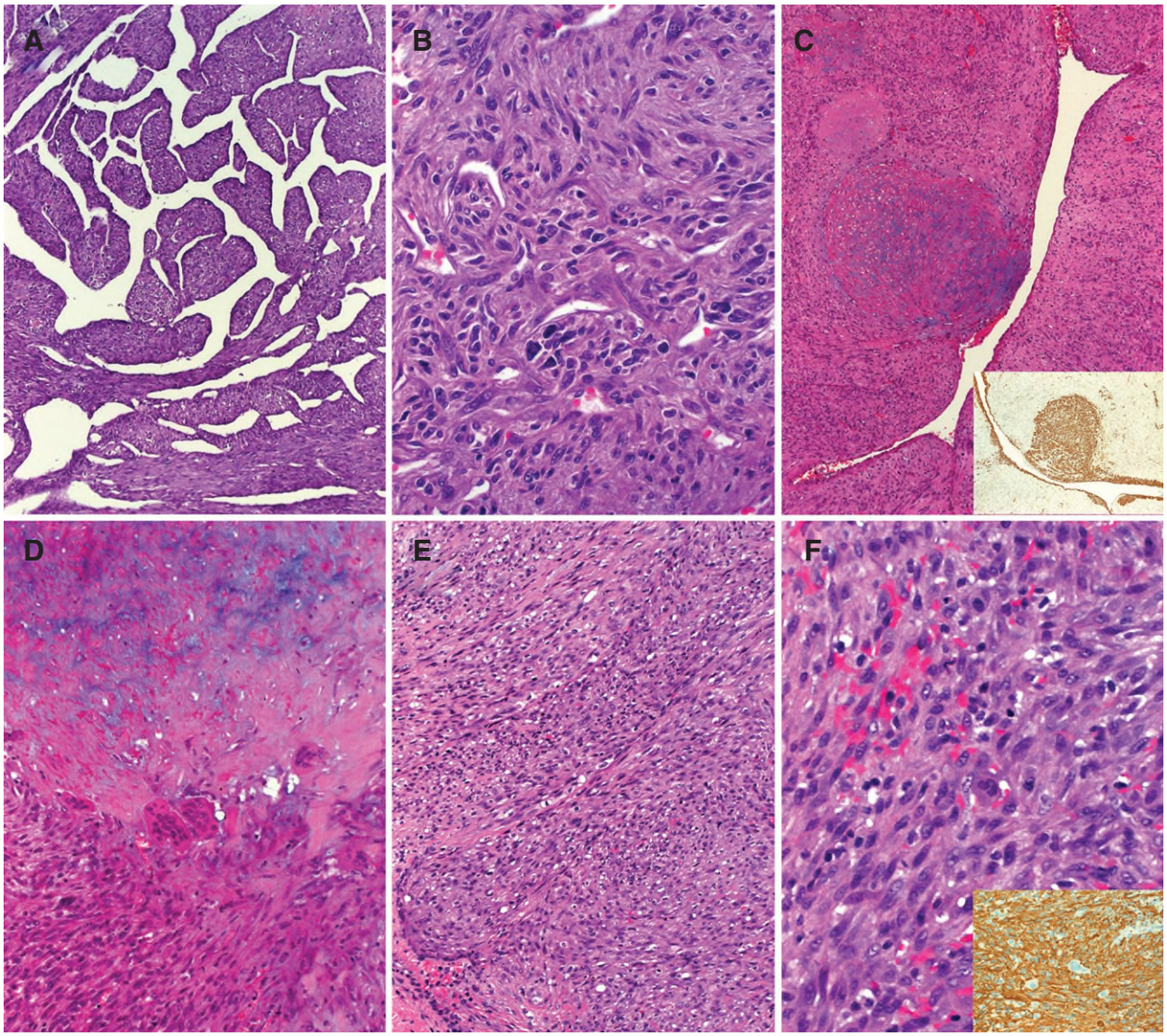

Figure 4. Histological features of paediatric cases with *NTRK1* fusion. (A) Extensive haemangiopericytic pattern with cystic dilated vascular gaps encasing tumour cells in Case 1. (B) Higher magnification showed plump spindle cells with mild atypia. (C) Ectatic vessels with associated myo-intimal nodules (vessel balls) were a frequent feature in the paediatric cases; (inset) smooth muscle actin stain. (D) These nodules were occasionally bordered by multinucleated giant cells. (E) Case 2 showed compact cellular fascicles of atypical spindle cells with prominent compressed vascular spaces. (F) A few multinucleated giant cells were seen at higher magnification; (inset) smooth muscle actin stain

genes observed in *NTRK1* gene fusions within papillary thyroid cancer comprise *TPM3*, *TP3* and *TFG* [12], but at least 10 additional 5′ partner genes have been reported [10], including *LMNA–NTRK1* gene fusions observed in spitzoid naevi/melanomas and soft tissue sarcomas [11].

Very recently, Doebele *et al* [9] reported on the dramatic response to a TrkA kinase inhibitor in a 41 year-old female patient with a *NTRK1* gene fusion-positive sarcoma with multiple lung metastases, and clinical trials addressing patients with tumours harbouring *NTRK1* gene fusions are currently ongoing. Interestingly, three of five *NTRK1* gene fusion-positive sarcomas from that study [9], as well as three of four cases from the current series, harboured additional *CDKN2A* deletions. Together with the amplification of the *NTRK1* fusion gene observed in our fourth case lacking a *CDKN2A* deletion, and incorporating the additional genetic aberrations observed in our index case analysed by whole-genome sequencing, these findings indicate that *NTRK1* gene fusions probably depend on further oncogenic events to be fully capable of inducing a soft tissue sarcoma. This idea was supported by increased viability in our cell model with *LMNA–NTRK1* gene fusion, with either additional p16 knock-down or transduction with increased *LMNA–NTRK1* copies/cell. Interestingly, the gains of whole chromosomes 8, 11, 12 and 20 observed in the paediatric index case by whole-genome sequencing in our study correspond well to a previous report on non-random gains of chromosomes 8, 11, 17 and 20 in infantile fibrosarcomas [26].

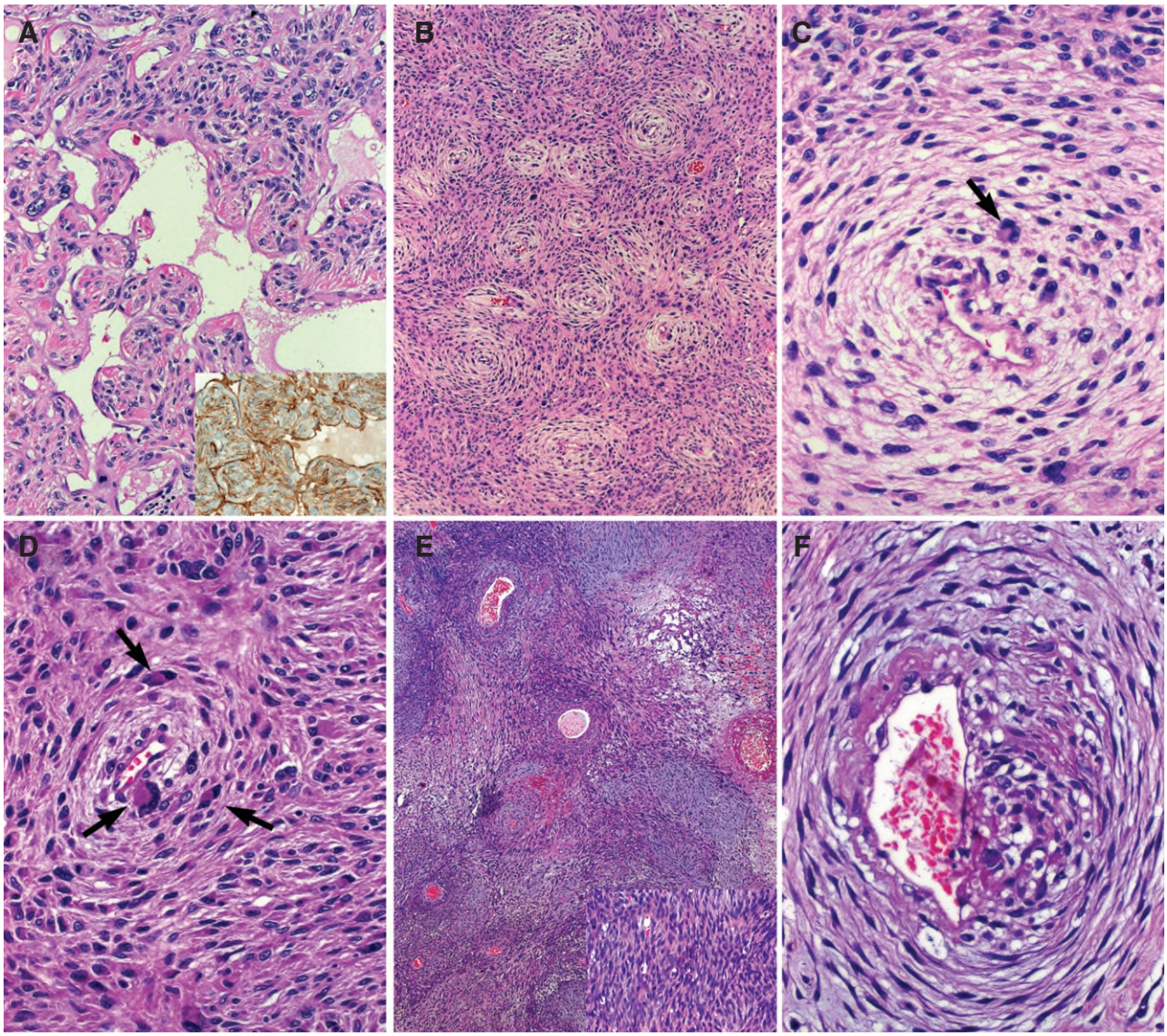

Figure 5. Histological features of adult cases with *NTRK1* fusion. (A) Case 3 showed a prominent haemangiopericytic pattern; note clear-cut nuclear atypia; (inset) CD34 stain. (B) Prominent myopericytoma-like growth in same case. (C, D) Higher magnification showing mild atypia in subendothelial cells and scattered larger eosinophilic binucleate tumour cells within the vascular wall (arrows). (E) Case 4 showed similar features but with higher cellular and focal compact fascicular growth (inset). (F) Higher magnification of myopericytic pattern showing characteristic obliterative vasculopathic-like tumour growth

Regarding the frequency of *NTRK1* gene fusions in sarcomas, Doebele *et al* [9] screened a total of 1272 soft tissue sarcomas and found only five cases with *NTRK1* gene fusions, including three tumours arising in children aged < 5 years. In that study, the three paediatric cases with *NTRK1* gene fusions were referred to as soft tissue Schwannoma (one case) or soft tissue fibrosarcoma (two cases), whereas the two adult cases were classified as soft tissue sarcoma, NOS [9]. The significant enrichment of *NTRK1* gene fusions among children aged < 5 years reported by these authors corresponds well to two of our four cases that were observed in children at the age of 11 months and 2 years. However, the probably low overall prevalence of *NTRK1* gene fusions among adult soft tissue sarcomas, which is far below 1% according to the study by Doebele *et al* [9], highlights the need for a histomorphologically guided screening to enable reasonable and specific testing for *NTRK1* gene fusion events in a routine diagnostic setting. Notably, most soft tissue sarcomas driven by specific gene fusions can be recognized by an experienced soft tissue pathologist through distinct histomorphological and immunohistochemical features. In contrast to the non-specific description of *NTRK1* gene fusion-positive soft tissue sarcomas in previous studies [9,25], we report for the first time on specific histomorphological features, including myo/haemangiopericytic pattern, in soft tissue sarcomas with *NTRK1* gene fusions. Our observation will help to identify sarcomas that have a much higher chance of carrying a *NTRK1* gene fusion compared to the very low percentage reported previously in an unselected cohort [9]. A reasonable chance for a positive test result is essential for substantial testing frequencies in a clinical routine setting. In particular, we did not perform

Table 1. Clinicopathological and immunohistochemical features of *NTKR1* fusion-positive sarcomas ($n = 4$)

Case	Age/ gender	Site	Size/mitotic counts/10 HPFs	Treatment	Outcome	Histological pattern	*NTRK1/CDKN2A* FISH	RT–PCR gene fusion	ASMA	Desmin	h-CD	CD34	STAT6	EMA	Pan-CK
1	2 yr/F	Paravertebral lumbar	14 cm/12	R2 excision radiotherapy with complete response	ANED (32 mo)	Infantile HPC-like sarcoma	Single red/loss	*LMNA–NTRK1*	focal+, MIP+	-	-, (MIP+)	-	-	-	-
2	11 mo/M	Back	3 cm/17	Complete excision	ANED (24 mo)	Myofibroblastic sarcoma-like	Inversion/loss	*TPM3–NTRK1*	+++	-	-	-	-	-	-
3	80 yr/M	Upper arm	6 cm/14	Complete excision, no adjuvant therapy	NA (recent case)	MPC-like sarcoma	Amplification of single red/intact	NA	-	-	-	++	-	NA	-
4	51 yr/F	Supraclavicular	6.5 cm/16	Complete excision, no adjuvant therapy	ANED (29 mo)	MPC-like sarcoma	inversion/loss	*TPM3–NTRK1*	-	-	-	-	-	focal+	++

F, female; M, male; yr, years; mo, months; HPF, high-power fields; ANED, alive with no evidence of disease; NA, not available; HPC, haemangiopericytoma; MPC, myopericytoma; h-CD, h-caldesmon; MIP, myointimal proliferations; Pan-CK, pan-cytokeratin AE1/AE3.

a blind search for *NTRK1* fusion-positive sarcoma, but tested a small cohort of sarcomas with morphological features guided by our index case. Our results suggest over-representation of *NTRK1* fusion-positive sarcoma among soft tissue sarcomas characterized by a prominent pericytic growth pattern but not fitting any defined sarcoma subtype. Thus, this study provides a novel molecular genetic event that will help to better clarify the until now not-well defined category of neoplasms with myopericytomatous pattern, and to separate them from related tumours with a distinct molecular genetic basis, eg infantile myofibromatosis with *PDGFRB* mutations [16,17].

In summary, we reported on recurrent *NTRK1* gene fusions in low-grade paediatric and adult soft tissue sarcomas unified by a prominent infantile HPC-like or myopericytoma-like growth pattern. Histomorphological homology of the cases in this small series suggests a potential disease entity with a varying spectrum. Future studies on larger series are needed to clarify whether the emerging group of sarcomas with *NTRK1* gene fusions will be best defined by the molecular genetic background (eg undifferentiated sarcoma with *NTRK1* gene fusion, in analogy to the *CIC–DUX4*-positive undifferentiated sarcoma), or whether the characteristic myopericytoma-like features described in the current manuscript substantiate the description of a novel morphologically and genetically defined soft tissue sarcoma entity. Our study underlines the necessity to test any sarcomatous neoplasm with similar features for *NTRK1* gene fusion. This is particularly relevant given the availability of novel effective targeted therapies for tumours with similar genetic alterations.

Addendum

During the review process of this manuscript, Wong and colleagues published a case of a congenital infantile fibrosarcoma with *LMNA–NTRK1* gene fusion in a 1 month-old child that showed a remarkable response to the tyrosine kinase inhibitor crizotinib [27]. They described the histomorphology of their case as a 'dense proliferation of spindle cells in herringbone pattern' and reported on positive CD34 immunostaining; however, no detailed morphological description or picture was presented. Altogether, their case is in line with our two paediatric cases and emphasizes the potential benefit of *NTRK1* gene fusion testing in tumours falling within the spectrum of infantile myofibromatosis/infantile HPC and congenital/infantile fibrosarcoma.

Acknowledgements

We thank Daniela Renner and Ute Zimmermann (Institute of Pathology, University Hospital Erlangen) and Ute Ernst [Sequencing Core Facility German Cancer Research Centre (DKFZ), Heidelberg] for excellent technical assistance.

Author contributions

FH and AAg conceived the study and wrote the manuscript; SW supervised the whole-genome and RNA sequencing analysis; MB, KK and MS analysed the sequencing data; JG and FH performed the FISH analysis; JK, AAc, EAM and RW conceived and performed the functional assays; AAS, IEA, AH and AAg contributed cases; and RC, OR and MM were involved in the treatment of the patients. All authors read and confirmed the final version of the manuscript.

References

1. Gengler C, Guillou L. Solitary fibrous tumour and haemangiopericytoma: evolution of a concept. *Histopathology.* 2006; **48:** 63–74.
2. Robinson DR, Wu YM, Kalyana-Sundaram S, *et al.* Identification of recurrent *NAB2–STAT6* gene fusions in solitary fibrous tumor by integrative sequencing. *Nat Genet* 2013; **45:** 180–185.
3. Chmielecki J, Crago AM, Rosenberg M, *et al.* Whole-exome sequencing identifies a recurrent *NAB2–STAT6* fusion in solitary fibrous tumors. *Nat Genet* 2013; **45:** 131–132.
4. Barthelmess S, Geddert H, Boltze C, *et al.* Solitary fibrous tumors/hemangiopericytomas with different variants of the *NAB2–STAT6* gene fusion are characterized by specific histomorphology and distinct clinicopathological features. *Am J Pathol* 2014; **184:** 1209–1218.
5. Agaimy A, Barthelmeß S, Geddert H, *et al.* Phenotypical and molecular distinctness of sinonasal haemangiopericytoma compared to solitary fibrous tumour of the sinonasal tract. *Histopathology* 2014; **65:** 667–673.
6. Haller F, Bieg M, Moskalev EA, *et al.* Recurrent mutations within the amino-terminal region of β-catenin are probable key molecular driver events in sinonasal hemangiopericytoma. *Am J Pathol* 2015; **185:** 563–571.
7. McMenamin ME, Fletcher CD. Malignant myopericytoma: expanding the spectrum of tumours with myopericytic differentiation. *Histopathology* 2002; **41:** 450–460.
8. Knezevich SR, McFadden DE, Tao W, *et al.* A novel *ETV6–NTRK3* gene fusion in congenital fibrosarcoma. *Nat Genet* 1998; **18:** 184–187.
9. Doebele RC, Davis LE, Vaishnavi A, *et al.* An oncogenic NTRK fusion in a soft tissue sarcoma patient with response to the tropomyosin-related kinase (TRK) inhibitor LOXO-101. *Cancer Discov* 2015; **5:** 1049–1057.
10. Vaishnavi A, Le AT, Doebele RC. TRKing down an old oncogene in a new era of targeted therapy. *Cancer Discov* 2015; **5:** 25–34.
11. Wiesner T, He J, Yelensky R, *et al.* Kinase fusions are frequent in Spitz tumours and spitzoid melanomas. *Nat Commun* 2014; **5:** 3116.
12. Greco A, Miranda C, Pierotti MA. Rearrangements of *NTRK1* gene in papillary thyroid carcinoma. *Mol Cell Endocrinol* 2010; **321:** 44–49.
13. Vaishnavi A, Capelletti M, Le AT, *et al.* Oncogenic and drug-sensitive NTRK1 rearrangements in lung cancer. *Nat Med* 2013; **19:** 1469–1472.
14. Mentzel T, Calonje E, Nascimento AG, et al. Infantile hemangiopericytoma versus infantile myofibromatosis. Study of a series suggesting a continuous spectrum of infantile myofibroblastic lesions. *Am J Surg Pathol* 1994; **18:** 922–930.
15. Variend S, Bax NM, van Gorp J. Are infantile myofibromatosis, congenital fibrosarcoma and congenital haemangiopericytoma histogenetically related? *Histopathology.* 1995; **26:** 57–62.
16. Cheung YH, Gayden T, Campeau PM, *et al.* A recurrent *PDGFRB* mutation causes familial infantile myofibromatosis. *Am J Hum Genet* 2013; **92:** 996–1000.
17. Martignetti JA, Tian L, Li D, *et al.* Mutations in *PDGFRB* cause autosomal-dominant infantile myofibromatosis. *Am J Hum Genet* 2013; **92:** 1001–1007.
18. Sadow PM, Priolo C, Nanni S, *et al.* Role of *BRAF* V600E in the first preclinical model of multifocal infiltrating myopericytoma development and microenvironment. *J Natl Cancer Inst* 2014; DOI: 10.1093/jnci/dju182.
19. Linos K, Carter JM, Gardner JM, *et al.* Myofibromas with atypical features: expanding the morphologic spectrum of a benign entity. *Am J Surg Pathol* 2014; **38:** 1649–1654.
20. Dictor M, Elner A, Andersson T, *et al.* Myofibromatosis-like hemangiopericytoma metastasizing as differentiated vascular smooth-muscle and myosarcoma. Myopericytes as a subset of 'myofibroblasts'. *Am J Surg Pathol* 1992; **16:** 1239–1247.
21. Arévalo JC, Wu SH. Neurotrophin signaling: many exciting surprises! *Cell Mol Life Sci* 2006; **63:** 1523–1537.
22. Martin-Zanca D, Hughes SH, Barbacid M. A human oncogene formed by the fusion of truncated tropomyosin and protein tyrosine kinase sequences. *Nature* 1986; **319:** 743–748.
23. Kim J, Lee Y, Cho HJ, *et al.* NTRK1 fusion in glioblastoma multiforme. *PLoS One* 2014; **9:** e91940.
24. Wu G, Diaz AK, Paugh BS, *et al.* The genomic landscape of diffuse intrinsic pontine glioma and pediatric non-brainstem high-grade glioma. *Nat Genet* 2014; **46:** 444–450.
25. Stransky N, Cerami E, Schalm S, *et al.* The landscape of kinase fusions in cancer. *Nat Commun* 2014; **5:** 4846.
26. Schofield DE, Fletcher JA, Grier HE, *et al.* Fibrosarcoma in infants and children. *Application of new techniques. Am J Surg Pathol* 1994; **18:** 14–24.
27. Wong V, Pavlick D, Brennan T, *et al.* Evaluation of a congenital infantile fibrosarcoma by comprehensive genomic profiling reveals an *LMNA–NTRK1* gene fusion responsive to crizotinib. *J Natl Cancer Inst* 2015; **108:** 1.

SUPPLEMENTARY MATERIAL ON THE INTERNET

The following supplementary material may be found in the online version of this article:

Figure S1. Copy number variations in the index case

Figure S2. RT–PCR validation of *LMNA–NTRK1* and *TPM3–NTRK1* gene fusions

Figure S3. Clinicopathological presentation of the index case

Table S1. RT–PCR primer sequences

Table S2. Expected product sizes for *LMNA–NTRK1* and *TPM3–NTRK1* gene fusions